Low-Energy Ion-Beam Etching

James R. Kahn and Harold R. Kaufman
Kaufman & Robinson Inc., Fort Collins, CO 80524

ABSTRACT

Etch-rate profiles have been obtained for copper, tantalum, stainless steel and quartz using a commercial end-Hall ion source. These profiles can be used to predict uniformity and etch rates in practical etching configurations. Compared to a gridded ion source, the lower ion energy of an end-Hall ion source is offset in etching rate by its large ion-current capacity, while the lower ion energy can be a significant advantage in damage-sensitive etching applications.

INTRODUCTION

End-Hall ion sources are widely used for in-situ cleaning and ion assisted deposition, which are necessary in many thin-film processes. Compared to gridded ion sources with expensive and complicated high-maintenance grids, end-Hall ion sources have the natural advantages of lower cost, broad ion-beam coverage, and greater reliability. End-Hall ion sources also have much larger ion-current capabilities at low ion energies (200 eV and less) permitting useful etch rates at these low energies and reducing or avoiding the damage that would otherwise occur to the surface being etched.[1] There are, however, limited etch data for this low energy range. The argon ion beam from an end-Hall ion source was used to generate both low-energy sputter yields and etch-rate profiles for copper, tantalum, type 304 stainless steel, and quartz. The etch profiles were used to predict uniformity and etch rates for etching apparatus with a single-rotation stage or a large single-rotation substrate. Excellent uniformity can be obtained at useful etch rates with the ion-source location selected by this procedure. The practical considerations of interactions with the vacuum-chamber wall are also addressed.

ION-BEAM CHARACTERIZATION

A commercial end-Hall ion source[2,3] was used for the etching described herein. The ion-beam profile and on-axis retarding potential energy analysis are shown in Fig. 1 for a discharge voltage and current of 150 V, 5.7 A. The working gas was argon and the background pressure was 2×10^{-4} Torr. These characteristics were obtained using an ion-beam probe, the design and use of which is described in a previous publication.[4] To minimize vignetting errors of the probe screen, the data for the profile in Fig. 1(a) were obtained with the probe facing, and kept a constant distance from, the center of the ion-source exit plane. Data from both sides of the ion-beam axis are plotted in Fig. 1(a), with the small differences in data at angles greater than zero indicating an essentially axisymmetric beam profile. The etch measurements were obtained at a flat plane oriented normal to the ion-beam axis (see Fig. 2). The profile that would be expected at such a flat plane would be reduced by the cube of the cosine of the angle from the axis, and is shown by the dashed line in Fig. 1(a). (The square of the cosine results from the inverse-square reduction due to increased distance, while an additional cosine results from the reduction due to the oblique incidence of the ions on the etched surface.)

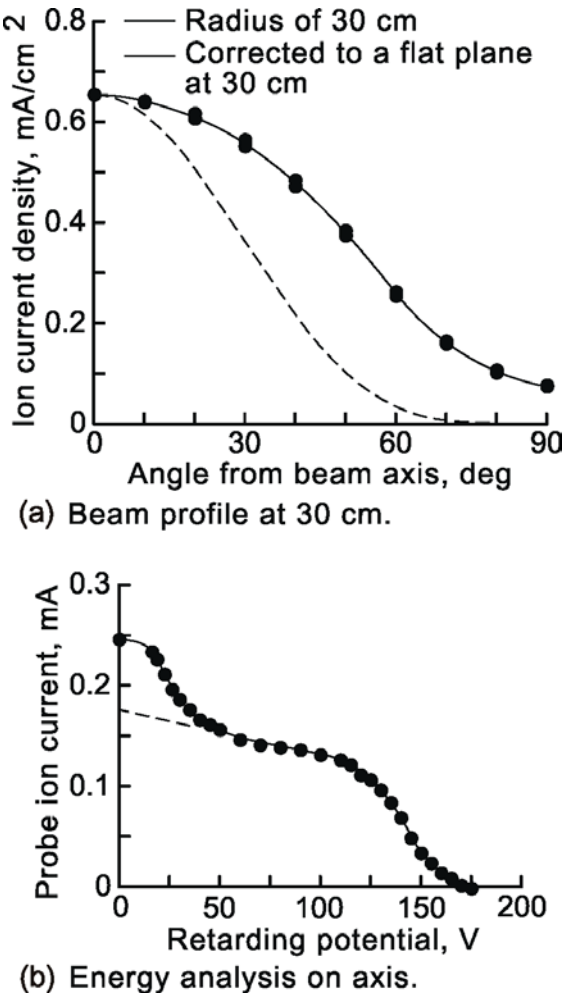

Figure 1. Ion-beam characteristics.

The retarding potential energy analysis on the ion source axis is shown in Fig. 1(b) for the same operating conditions. This plot shows the ion current reaching the probe over a range of positive probe potentials. The slope of this curve at a given potential indicates the density of the ion current with energies near that potential. (The curve would have to be differentiated to show the actual energy distribution of the ions.) The shape of the curve in Fig. 1(b) indicates large numbers of ions with energies near 25 and 150 eV, with smaller numbers distributed between. The ions near 25 eV are mostly charge-exchange ions,[4] generated when energetic beam ions pass near background neutrals, although ion-source design or operation can also contribute to the density of these low energy ions. The ions closer to 150 eV are those that provide most of the ion-beam processing capability. The mean energy can be obtained from the area under the retarding-potential curve and is about 89 eV for the curve shown by the data. If the contribution from charge-exchange ions (above the dashed line) is excluded, the mean ion energy increases to 114 eV.

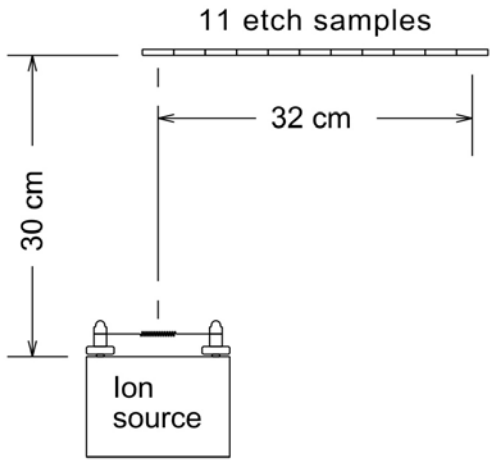

Figure 2. Configuration used for etch-rate profiles.

ETCH-RATE PROFILES

The configuration used to measure etch-rate profiles is indicated in Fig. 2. Etch samples were placed in a plane normal to the ion-source axis at a distance of 30 cm from the source. Because of the beam symmetry shown in Fig. 1(a), etch measurements were made on only one side of the ion beam. The samples were 32 mm square with smooth surfaces. The etch measurements were calculated using electronic-scale weight measurements, the material density, and the exposed area. Step measurements with a stylus profilometer were used to verify the procedure used. The run times were adjusted to be long enough to avoid effects of surface anomalies such as native oxides and short enough to avoid any significant effect of texturing. Checks were also made to assure that sputtering from other hardware in the configuration of Fig. 2 did not affect the etch rate measurements.

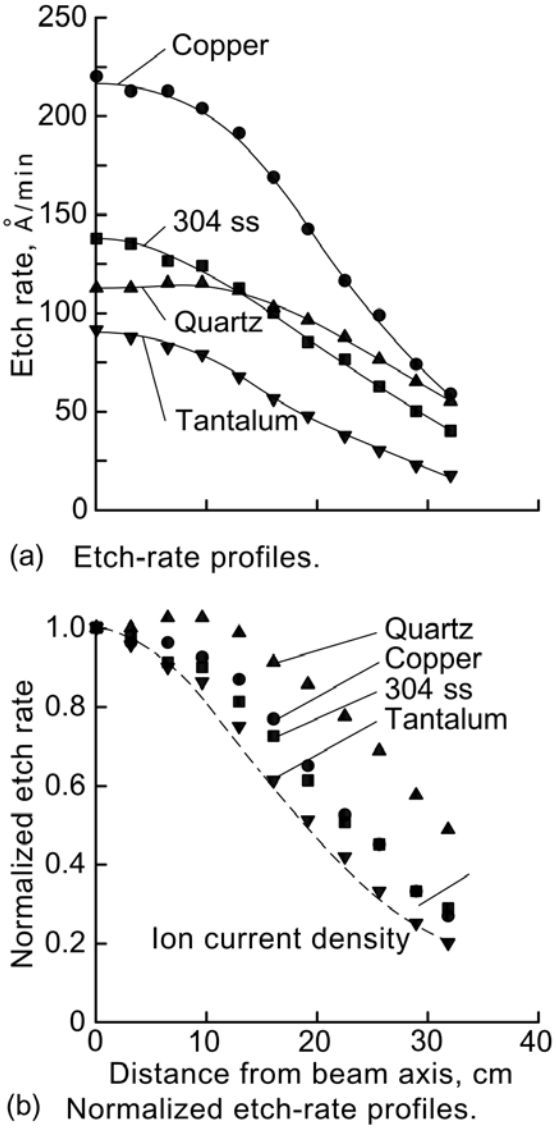

Figure 3. Etch-rate profiles.

Etch-rate profiles were obtained with copper, tantalum, 304 stainless steel, and quartz samples and are shown in Fig. 3(a). Using the current density and etch rates on axis (normal incidence), the sputter yields in atoms/ion for copper, tantalum, stainless steel, and quartz are 0.76, 0.14, 0.49, and 0.31. The mean ion energy is roughly 100 eV (between 89 and 114 eV).

The same profiles were normalized to unity on the beam axis and are shown in Fig. 3(b), together with a normalized profile of ion current density obtained from the dashed line in Fig. 1(a). Referring to Fig. 3(b) and normalized parameters, the etch rates of all materials except tantalum increase above the ion current density and stay well above it as the angle increases from zero, indicating a substantial effect of the angle of incidence. The importance of angle of incidence is, of course, well known.[5] The magnitude of this effect, however, is often not available for the energies and materials of interest in a particular application.

EFFECT OF VACUUM-CHAMBER WALL

The etch profile obtained in a practical application can be affected by the proximity of the vacuum-chamber wall. A test configuration for demonstrating this interaction is shown in Fig. 4. Because the presence of the wall resulted in a nonsymmetrical etch distribution, the array of etch samples was centered relative to the ion source. The vacuum-chamber wall was simulated with a sheet of 304 stainless steel. The etch samples were made of the same material as the simulated vacuum-chamber wall to simplify the analysis of the test results. The baffles were also made of 304 stainless steel sheet, although this material is not as important because the etch samples do not "see" the surface of the baffle that is sputtered.

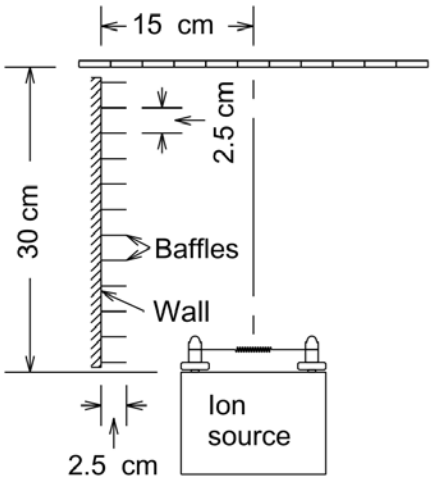

Figure 4. Configuration used to measure wall effect.

The wall-interaction test sequence consisted of three tests with the ion source operating at the same conditions as described in connection with Fig. 1. The first test was with no wall or baffle present. The second test was with only the simulated vacuum-chamber wall present. The third test was with both wall and baffles present. The etch-rate profiles for these three tests are shown in Fig. 5. The profile without wall or baffle establishes the basic etch-rate profile and is not significantly different from the 304 stainless steel profile in Fig. 3. The etch-rate profile with only the wall present shows the reduced etching of samples near the wall due to the deposition of sputtered material from the wall. The difference between these two profiles gives the deposition from the wall shown by the curve at the bottom of Fig. 5. The scatter is substantial for these deposition data because they were obtained from difference measurements. The deposition also included contamination from wall impurities, which in turn resulted in a dull, textured surface, which also affected the etch rate. Even so, the effect of wall deposition is clearly seen to extend over most of the samples. The etch-rate profile with both the wall and the baffles present shows that the sputtering from the wall is essentially avoided and the normal etch profile is obtained quite close to the wall. This profile falls off only where the samples are shadowed by the baffles.

Although Fig. 5 is presented here in the context of etching, it should be apparent that it also has significance for controlling contamination in ion assist applications.

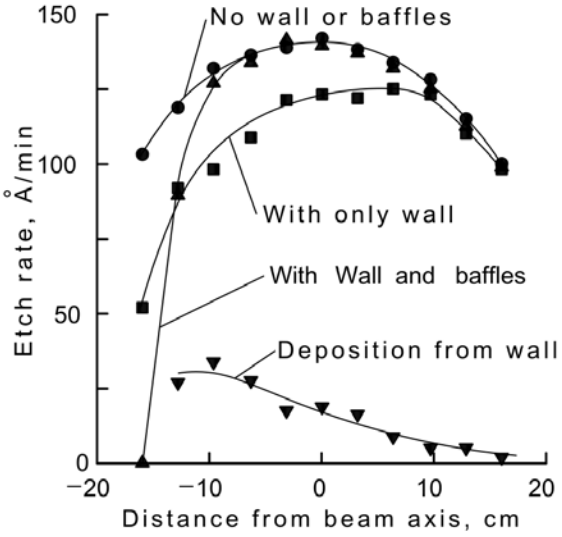

Figure 5. Etch-rate profiles showing the wall effect and its control.

UNIFORMITY FOR SINGLE-ROTATION STAGE

Single-rotation stages with multiple substrates or the single-rotation of large wafers or substrates are both widely used for thin-film processing. A numerical modeling procedure was used predict etch uniformity for such a configuration. This procedure assumed a planar etched region and divided this region into 20 radial zones and averaged over 72 equally spaced circumferential locations for each of these zones. The shape of the etch-rate profile at the planar surface being etched (fig. 3) was assumed to be of the form $\cos^x\Theta$, where Θ is the angle from the beam axis and where x = n+3 for a planar surface and n is the shape parameter and Θ is the angle from the beam axis. This formalism has been used to describe the shape of end-Hall ion beams[6] and is extended here to the etch profile of such a beam. Because the calculation numerically integrates contributions from a wide range of relative substrate-beam locations, the effects of moderate departures from the ideal $\cos^x\Theta$ shape should be small. While the etched surface was assumed to be planar, the calculations should also be approximately correct for small departures from a planar shape.

The magnitude of the shape parameter for the etch profile can be determined from Fig. 1, using the half-amplitude half-angle. For both copper and stainless steel, this angle is about 38 degrees and x equals about 2.9. That is, $(\cos 38^\circ)^{2.9} \approx 0.5$. Using the definition for shape parameter for a flat surface[6], n = -0.1. The etch profile for these two metals is significantly flatter than the ion-beam profile that generates the etching, as shown in Fig. 3(b). The half-amplitude half-angle for the ion beam is about 32 degrees and its shape parameter, n, is about +1.2.

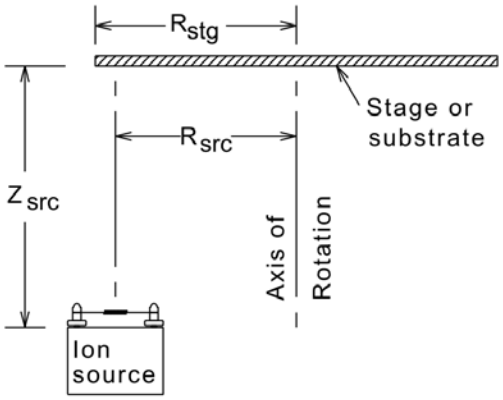

Figure 6. Single-rotation etching configuration.

For a given stage (or single substrate) radius, R_{stg}, the radius at which the source is located, R_{src}, was varied to give the best uniformity, (max-min)/(max+min), in percent. The mean etch rate, (max+min)/2), is given as a percent of the nominal etch rate, which is the etch rate on-axis for a stationary substrate at a distance of 30 cm (220 Å/min for copper and 140 Å/min for 304 stainless).

Table 1 is for a source distance, Z_{src}, of 30 cm and a shape parameter, n, of –0.1. For a stage radius, R_{stg}, of 30 cm, for example, the optimum radius of the ion source, R_{src}, for uniformity is 32 cm, for which the uniformity is ±2.5% and the mean etch rate is 34% of nominal. For copper this would be a mean etch rate of 0.34×220 = 75 Å/min. Uniformities and etch rates for source distances, Z_{src}, other than 30 cm can be obtained by scaling all the distances simultaneously. For example, using the values in Table 1 for a stage radius of 35 cm, if all the dimensions were doubled, the stage radius, R_{stg}, would be 70 cm, the optimum source radius, R_{src}, would be 68.4 cm, and the source distance, Z_{src}, 60 cm. The uniformity would remain at 3.9%, but the etch rate would be decreased by a factor of 4 (four times the area to be etched) to about 8% of the nominal value. Careful examination of the options will show that, for a given stage radius, uniformity and etch rate can be exchanged by varying the source distance.

Table 1. Uniformity and etch rates for different stage radii, R_{stg}, at a source distance, Z_{src}, of 30 cm and with a shape parameter, n, of –0.1.

R_{stg}, cm	R_{src}, cm	Uniformity, ± %	Rate, % Nominal
25	30.0	1.4	37
30	32.0	2.5	34
35	34.2	3.9	31
40	36.6	5.8	28
45	39.0	7.9	26
50	41.7	10.3	23

To give a uniform etch, the axis of the ion beam generally must be directed near the outer edge of the area being etched (note R_{src} is roughly equal to R_{stg}). In many installations, this means that etching of the vacuum-chamber wall or other nearby hardware must be controlled with baffles. Selecting baffle locations is fairly straightforward and is based on preventing ion-beam impingement on surfaces that can "see" the surface being etched.

CONCLUDING REMARKS

An economical and reliable end-Hall ion source can be used for an etching application where a substantial amount of material must be removed from a large area. Compared to a gridded ion source, the lower ion energy of an end-Hall ion source is offset in etching rate by its large ion-current capacity and broad coverage, while the lower ion energy can be a significant advantage in etching applications that are sensitive to damage caused by energetic ions. The broad ion beam of an end-Hall ion source is well suited to uniform etching over large areas although care may be required to control the effects of etching nearby vacuum-chamber walls or other hardware.

REFERENCES

1. H.R. Kaufman and J.M.E. Harper, "Ion-Assist Applications of Broad-Beam Ion Sources," *Proceedings of SPIE*, 5527, 50, 2004.

2. EH1000 filament ion source, Kaufman & Robinson, Inc., Fort Collins, CO 80524.

3. H.R. Kaufman, *U.S. Pat. #6,608,431*, "Modular Gridless Ion Source," Aug. 19, 2003.

4. J.R. Kahn, H.R. Kaufman, R.E. Nethery, R.S. Robinson, and C.M. Shonka, "Low-Energy End-Hall Ion Source Characterization at Millitorr Pressures," *48th Annual Technical Conference Proceedings of the Society of Vacuum Coaters*, 17, 2005.

5. G.K. Wehner and G.S. Anderson, "The Nature of Physical Sputtering," Chapt. 3 in *Handbook of Thin Film Technology*, McGraw-Hill Book Company, New York, 1970.

6. H.R. Kaufman and R.S. Robinson, pp. 65-66 in *Operation of Broad-Beam Sources,* Common-wealth Scientific Corporation, Alexandria, Virginia, 1984.